Case Report

Metastatic mucinous ovarian carcinoma simulating lung primary: an integrated diagnostic lesson

Giuseppe Pelosi[1,2], Marco De Luca[2], Maria Cannone[2], Emanuela Balladore[2], Isabella Ricotti[3], Davide Toniolo[4], Matteo Incarbone[5]

[1] Department of Oncology and Hemato-Oncology, University of Milan, Milan, Italy; [2] Inter-hospital Pathology Division, Istituto di Ricovero e Cura a Carattere Scientifico - IRCCS MultiMedica, Milan, Italy; [3] Division of Pathologic Anatomy and Histology, Azienda Socio-Sanitaria Territoriale Rhodense - Presidio Ospedaliero di Rho, Rho, Italy; [4] Division of Medical Oncology and Hematology, Azienda Socio-Sanitaria Territoriale Rhodense - Presidio Ospedaliero di Rho, Rho, Italy; [5] Division of Thoracic Surgery, Istituto di Ricovero e Cura a Carattere Scentifico - IRCCS MultiMedica, Milan, Italy

Summary

We herein document a rare instance of primary mucinous ovarian carcinoma metastatic to the left lung, whose deceptive secondary derivation was already envisaged according to the spectacular thromboembolism involving small pulmonary vessels, thereby realizing a centrifugal and centripetal metastatizing loop. This presentation was indicative of dismal prognosis. A multimodal biomarker key approach is herein emphasized, which included close clinico-pathologic data integration.

Key words: lung, ovary, mucinous adenocarcinoma, KRAS, G12C

Introduction

Comprehensive histologic assessment of lung cancer, immunohistochemistry (IHC) characterization and molecular profiling make up an effective triad to distinguish independent primary non-small cell carcinomas from intrapulmonary metastases [1,2]. However, scrutiny of the arterial, lymphatic and venous route for thromboembolic cancer cells represents a powerful tool to envisage the metastatic origin of tumors in the lung, either synchronous or metachronous [3]. This holds particularly true while facing with pulmonary invasive mucinous adenocarcinoma (PIMA), which is likely to share prototypical presentation of multiple/bilateral nodules [4], gastrointestinal-type IHC profiling (with TTF1 consistent negativity [1,5] and cyto-histologic features that are even commonly shared by mucin-laden extrapulmonary metastases [1]. The prognosis of patients with PIMA is a controversial subject with studies reporting a range of clinical outcomes where pneumonic infiltrates foresee poor behavior [4,6,7]. At variance with tumors originating in the gastrointestinal tract (pancreas, colon-rectum, stomach, appendix or biliary tree) [1], primary mucinous ovarian carcinoma (PMOC) rarely represents a source of malignancy to the lungs (PMOC is just 3% of all epithelial ovarian cancers [8] and 18% of all mucinous ovarian tumors) [9], which however deceptively straddles PIMA because of striking gastrointestinal-type histologic resemblance, common molecular traits and superimposable IHC profiling. Of note, however, 92% of PMOC are diagnosed in stage I disease [9] and extra-

ovarian dissemination to the lungs is quite uncommon, usually bearing unfavorable prognosis (overall survival is between 12 and 33 months) [8,9]. Therefore, the distinction between primary and secondary mucinous carcinoma may be demanding for practitioner pathologists, but is always clinically warranted. In this regard, pathologists may provide useful insights at the level of the microscopic evaluation of surgically resected specimens.

Case report

A 65-year-old Caucasian woman, current smoker, underwent in June 2021 radical left upper lobectomy, atypical resection of the left lower lobe and homolateral hilar-mediastinal extended lymphadenectomy because of three peripheral nodules sized 17 mm and 7 mm (upper lobe) and 10 mm (lower lobe), respectively. No other nodules were visible in the lungs at presentation (Fig. 1 A-B). Pathologic examination of all lung nodules featured mucin-laden goblet-to-columnar cancer cells organized in acinar and complex glandular patterns with labyrinthine growth appearance and foci displaying lepidic-like growth with cell tufting, which could be consistent with PIMA at a glance (Fig. 2 A-B). No significant necrosis was found in the three nodules. More accurate histological scrutiny, however, revealed massive centrifugal-type thromboembolism of small pulmonary arteries and their terminal branches, alveolar vessel permeation, massive pleural infiltration at the PL1 level, diffuse lymphatic vessel emboli, and pulmonary vein root permeation with centrifugal-type escape alongside interacinar and interlobular septa far from the centrilobular bronchovascular bundles (Fig. 2 C-H). No thromboembolism of major branches of pulmonary arteries was detected. Mediastinal lymphadenectomy confirmed, on histologic sections, the extensive N1 and N2 metastatic involvement suggested by imaging (Fig. 1 B).

An IHC study showed strong and diffuse decoration for PIMA-related markers, such as HNF4-alpha, MUC5AC, CK7, CK20 and CDX2, as well as consistent negativity for TTF1 [1,5]. Despite the close histologic resemblance to multifocal PIMA, pulmonary vessel involvement with extensive carcinomatous arteriopathy, diffuse interstitial capillary and lymphatic permeation, pleura vessel invasion and massive pulmonary vein thromboembolism pushed the final diagnosis of metastatic IMA in the left lung to be envisaged. This peculiar pulmonary presentation, however, prompted us to clinically search for a possible primary tumor elsewhere, which revealed that the patient had been operated in April 2020 for a stage-I right PMOC (sized 15x24x25 cm), featuring intestinal-type differentiation, mural nodules of sarcomatoid carcinoma, remnants of borderline mucinous tumor and benign Brenner tumor, upon revision (Fig. 2 I-J). A comparative histologic and IHC study confirmed the same features as those detected in the three pulmonary nodules, which however lacked any sarcomatoid component. Additional p53 immunostaining in both anatomical sites showed diffuse and strong nuclear decoration of tumor cells, supportive of *TP53* gene mutation status (no Sanger or next generation sequencing was available in our laboratory) (Fig. 2 K-L). A molecular study for *KRAS* by real-time PCR (Idylla KRAS Mutation Test, Biocartis NV, Mechelen, Belgium) revealed the same G12C mutation (34G > T) in both ovarian (including mural nodules of sarcomatoid carcinoma) and pulmonary tumor growths, while a FISH study for *CDKN2A-p16* gene deletion did not reveal any alteration in either anatomical site.

The patient had undergone 6 courses of adjuvant chemotherapy with carboplatin in October 2020 for her initial PMOC and several additional courses of carboplatin and paclitaxel were administered after the diagnosis of pulmonary metastasis was rendered. The subsequent follow-up showed left pleural effusion for massive pleura recurrence and new bilateral lung nodules but not pneumonic infiltrates, which were further subjected to carboplatin and paclitaxel therapy and PARP-inhibitor niraparib (one tablet/day) treatment. At the end of January 2022, the patient began to experience mental confusion and march instability due to widespread central nervous system relapse in the frontal and occipital lobes and cerebellum, for which gamma-knife radiotherapy was undertaken along with best supportive care. The patient was then admitted to hospice until death a few weeks later, with massive thoracic and cerebral progression. A schematic interpretation of neoplastic dissemination route from the ovary to the lung and from the lung to systemic spread is exemplified in Figure 3.

Discussion

Our case is paradigmatic and instructive for at least three reasons, which are briefly discussed, thereby realizing an integrated diagnostic lesson useful in pathology practice.

a) The power of histologic assessment to figure out extrapulmonary derivation metastasis just on the basis of the massive loop-like involvement of small pulmonary vessels, despite cytologic, architectural and IHC features did not *a priori* rule out PIMA (the patient was also current smoker). As general rule, however, it
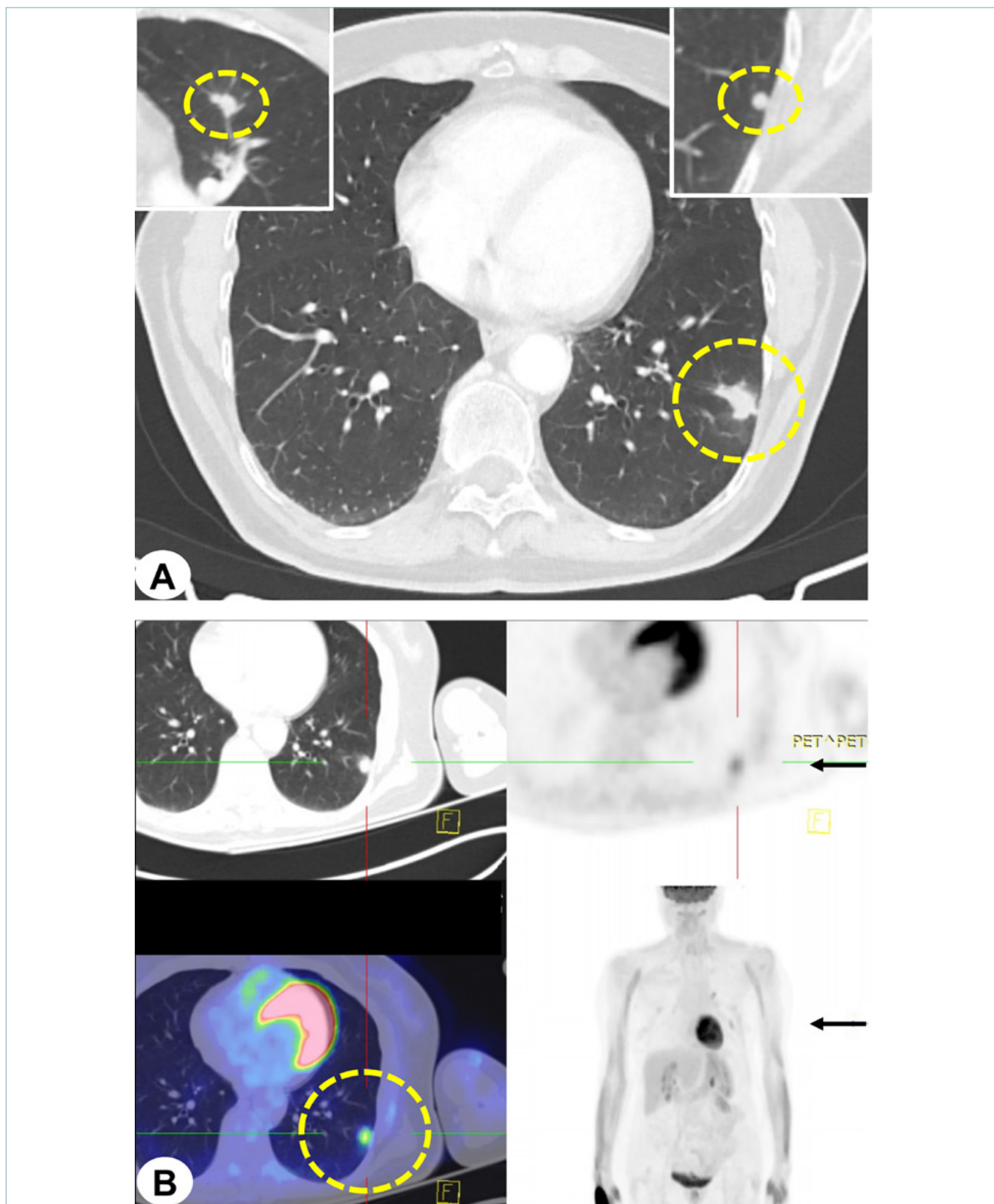
Figure 1. (A-B). Computed tomography scan examination revealed a 17 mm-sized nodule in the left upper lobe (dotted yellow circle), along with two additional nodules of 7 mm in the upper left lobe (upper right inset) and of 10 mm in the left lower lobe (upper left inset), respectively (A). Positron emission tomography reconstruction confirmed metabolic uptake in the largest nodule of the left upper lobe, whose position is double arrowed in black on the right (B).
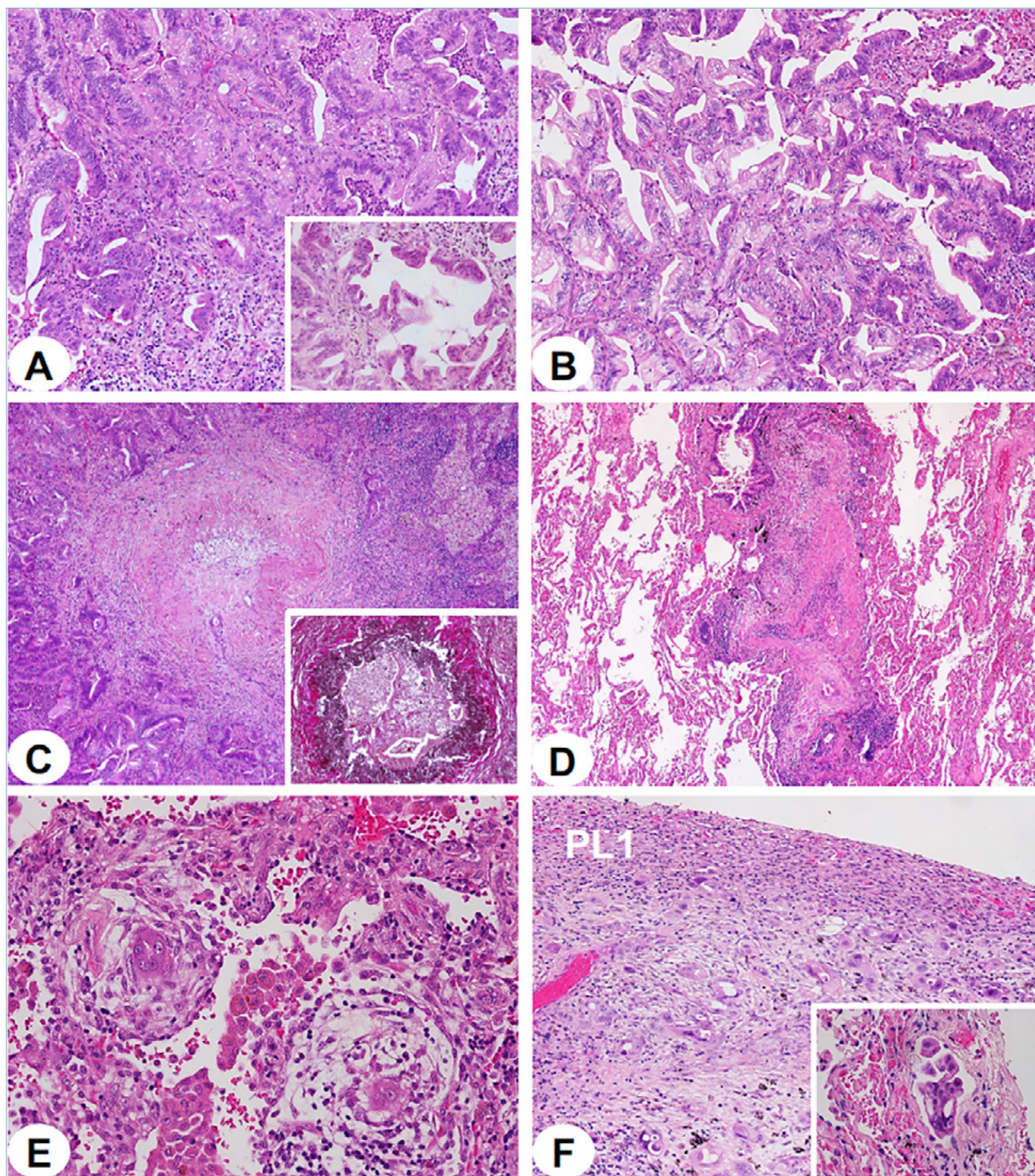
Figure 2. (A-F). In the lung, invasive mucinous adenocarcinoma featured acinar and complex glandular patterns with laby-rinthine growth appearance (A), lepidic-like growth (A, inset), goblet to columnar mucinous cells, basally located nuclei and gastrointestinal-type histologic appearance (B). Massive and multifocal carcinomatous thromboembolism was readily ob-served in all branching pulmonary arteries (elastin stain shows internal and external layers, inset) (C) and massively perme-ated their terminal branches along accompanying centrilobular bronchioles, thereby realizing a centrifugal-type colonization route (D). Even interstitial vascular channels were diffusely engulfed by cancer cells (E). Visceral pleural layer was infiltrated at the level PL1, with many tumor emboli accumulating with lymphatic vessels (F, inset).
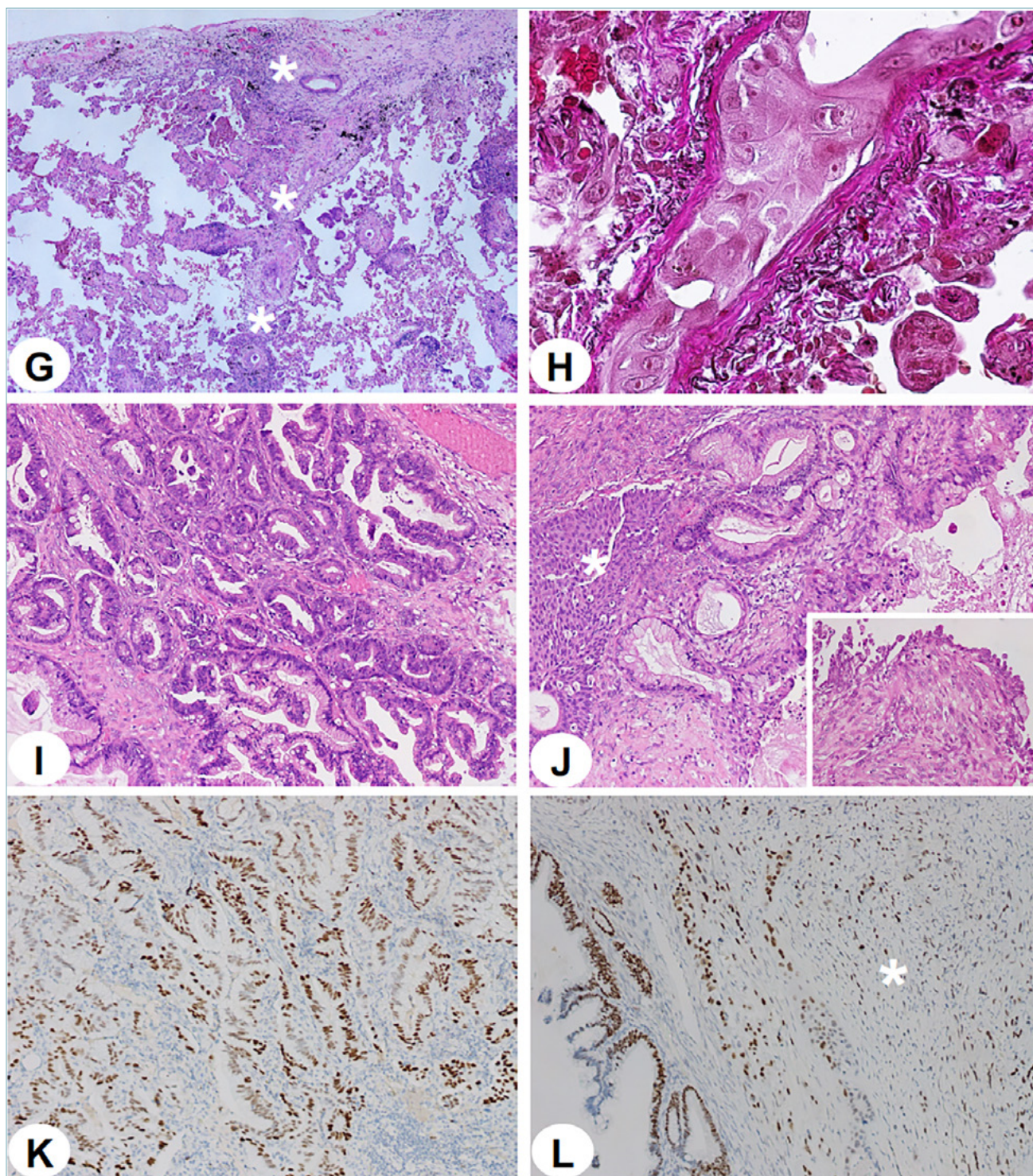
Figure 2. (G-L). The return loop of carcinomatous thromboembolism engulfed the pulmonary vein roots in the pleura, then running along interacinar and interlobular connective septa (G, white asterisks). Veins are hallmarked by a single external layer of elastic fibers (H). In the primary mucinous ovarian carcinoma, superimposable histologic features were seen with destructive stromal invasion (I), remnants of benign Brenner tumor (J, white asterisk) and sarcomatoid carcinoma mural nodules (J, inset). Tumors shared the same strong and diffuse decoration for p53, a surrogate marker of gene mutation, in both the lung (K) and the ovary including sarcomatoid carcinoma-looking mural nodules (L, white asterisk)

is worth stressing that any IMA diagnosis in the lung always requires accurate evaluation of the patient's clinical history, although the massive vascular involvement in our case was already supportive of metastatic derivation even before discovering the previous occurrence of a histologically similar ovarian cancer, even if it was apparently in early stage and nothing suggested a metastatic tumor (92% of PMOC are diagnosed
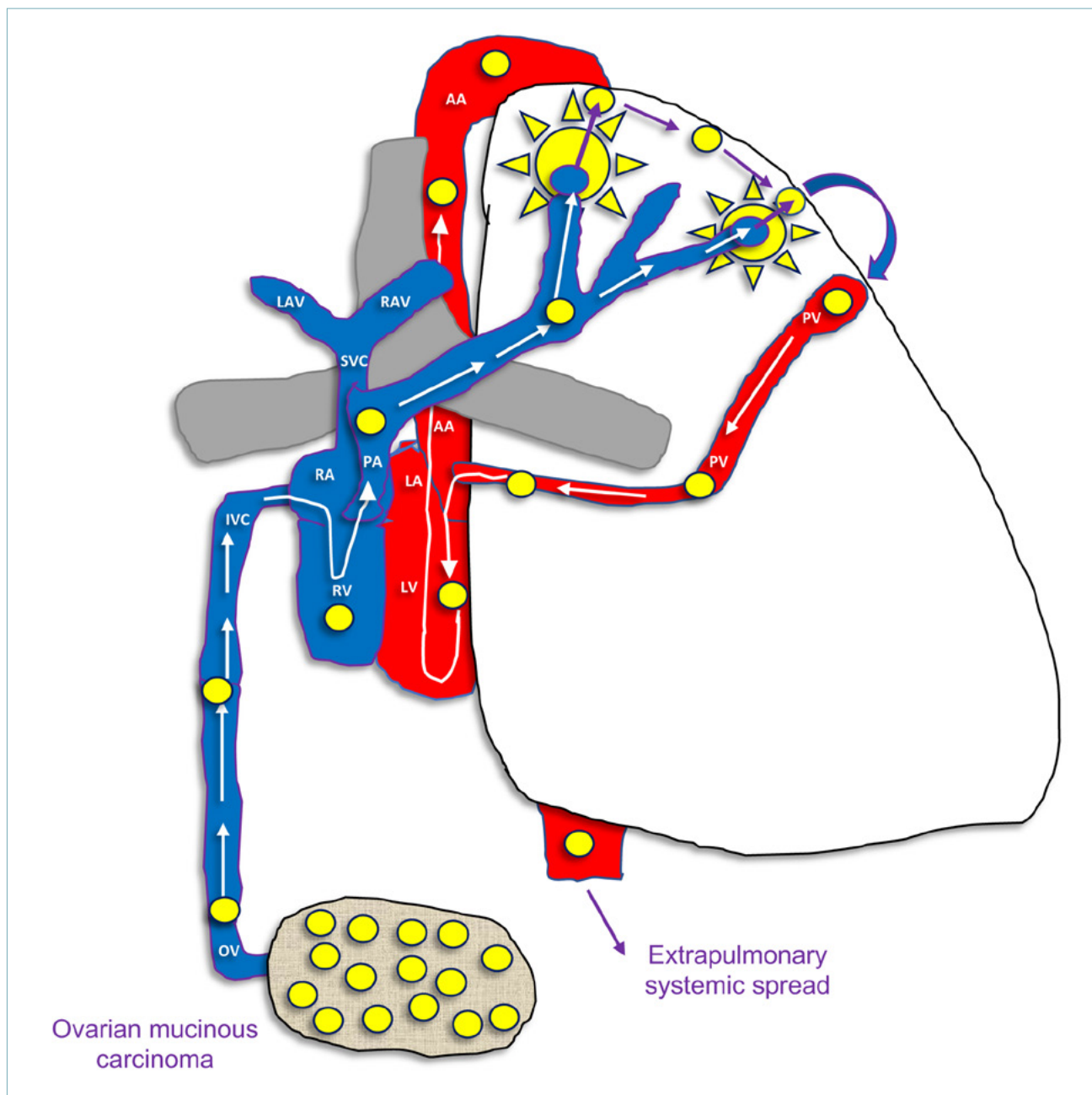

Figure 3. Schematic drawing of centrifugal and centripetal type dissemination inside the lung by primary mucinous ovarian carcinoma, with permeation of small pulmonary arteries. Major branches of pulmonary arteries and veins were free of neoplastic emboli. OV: ovarian vein; IVC: inferior cava vein; RA: right atrium; RV: right ventricle; PA: pulmonary artery; SVC: superior vena cava; LAV: left anonymous vena; RAV: right anonymous vena; LA: left atrium; LV: left ventricle; AA: ascending aorta; PV: pulmonary vein. Circles of either yellow or light blue color indicate embolic propagation by cancer cells, even at the pleura level. Arrows with heads suggest flow directions.

in stage I disease) [9]. This holds true even considering that IHC profiling is unlikely to be resolutive in the relevant differential diagnosis owing to striking decoration overlap, as well documented in our case.

b) The role of KRAS G12C mutation and hence the practical relevance to paying attention to the type of mutation in diagnostic molecular work-up (G12C is one of the least frequent mutations in PIMA [10-12] but the most prevalent mutation in PMOC) [13] and of p53 diffuse and strong immunostaining as a practical surrogate marker of mutation for comparison when sequencing is unavailable for whatever reason (*TP53* is mutated in 50 to 75% PMOC especially with destructive stromal invasion [8], while among the least frequent mutations in PIMA) [11]. *KRAS* mutation is thought to be an early event in PMOC formation [8] (it was present in both the glandular and sarcomatoid components of our case), whereas *TP53* is altered in the course of malignant transformation, was found in mural carcinomatous nodules too [14] (Fig. 2 K-L) and could be indicative of either epithelial-mesenchymal transition in the ovarian cancer progression [15] or mesenchymal-epithelial transition in the lung metastatic foci [16]. Of note, even spatially separate nodules in PIMA are clonally related to each other, just like extrapulmonary metastases [4], thus increasing the risk of diagnostic misinterpretation. Copy number loss of *CDKN2A* (*p16*), which is described in as many as 25-76% PMOC [8,13] but just in 20% of PIMA [11,17], was consistently absent in both anatomical sites of our case, thus confirming the relationship between pulmonary and ovarian tumors. The clinical evolution of *KRAS/TP53*-mutated metastatic PMOC is unfavorable (overall survival is between 12 and 33 months) [8,9], whereas *KRAS*-mutated PIMA has even been associated with lower pathological stage and absence of p53 protein overexpression [18].

c) The subsequent tumultuous clinical course with early thoracic and central nervous system relapse was predicted by the widespread centrifugal-type dissemination via pulmonary vein roots, which is infrequent in PIMA [1,4] that frequently grows multifocally, may produce pneumonia-like consolidations (infrequent in metastases probably due to their more tumultuous clinical course) and are frequently found in lower lobes [19]. As diagnosis of metastasis in the lung may be subtle and deceptive, emphasizing the role of comprehensive histologic assessment (also including the pattern and extent of vascular invasion) may be clinically warranted through a multimodal biomarker key approach.

References

1. Editorial Board: Borczuk C, Cooper W, Dacic S, et al. Thoracic tumours. International Agency for Research on Cancer. Lyon: IARC Press: 2021.

2. Girard N, Deshpande C, Lau C, et al. Comprehensive histologic assessment helps to differentiate multiple lung primary nonsmall cell carcinomas from metastases. Am J Surg Pathol 2009;33:1752-1764. https://doi.org/10.1097/PAS.0b013e3181b8cf03

3. Travis W, Nicholson A, Geisinger K, et al. Tumors of the Lower Respiratory Tract. AFIP; 2019.

4. Yang SR, Chang JC, Leduc C, et al. Invasive mucinous adenocarcinomas with spatially separate lung lesions: analysis of clonal relationship by comparative molecular profiling. J Thorac Oncol 2021;16:1188-1199. https://doi.org/10.1016/j.jtho.2021.03.023

5. Sonzogni A, Bianchi F, Fabbri A, et al. Pulmonary adenocarcinoma with mucin production modulates phenotype according to common genetic traits: a reappraisal of mucinous adenocarcinoma and colloid adenocarcinoma. J Pathol Clin Res 2017;3:139-152. https://doi.org/10.1002/cjp2.67

6. Casali C, Rossi G, Marchioni A, et al. A single institution-based retrospective study of surgically treated bronchioloalveolar adenocarcinoma of the lung: clinicopathologic analysis, molecular features, and possible pitfalls in routine practice. J Thorac Oncol 2010;5:830-836. https://doi.org/10.1097/jto.0b013e3181d60ff5

7. Lee HY, Cha MJ, Lee KS, et al. Prognosis in resected invasive mucinous adenocarcinomas of the lung: related factors and comparison with resected nonmucinous adenocarcinomas. J Thorac Oncol 2016;11:1064-1073. https://doi.org/10.1016/j.jtho.2016.03.011

8. Morice P, Gouy S, Leary A. Mucinous ovarian carcinoma. N Engl J Med 2019;380:1256-1266. https://doi.org/10.1056/NEJMra1813254

9. Riopel MA, Ronnett BM, Kurman RJ. Evaluation of diagnostic criteria and behavior of ovarian intestinal-type mucinous tumors: atypical proliferative (borderline) tumors and intraepithelial, microinvasive, invasive, and metastatic car-

cinomas. Am J Surg Pathol 1999;23:617-635. https://doi.org/10.1097/00000478-199906000-00001

10 Nakaoku T, Tsuta K, Ichikawa H, et al. Druggable oncogene fusions in invasive mucinous lung adenocarcinoma. Clin Cancer Res 2014;20:3087-3093. https://doi.org/10.1158/1078-0432.CCR-14-0107

11 Chang JC, Offin M, Falcon C, et al. Comprehensive molecular and clinicopathologic analysis of 200 pulmonary invasive mucinous adenocarcinomas identifies distinct characteristics of molecular subtypes. Clin Cancer Res 2021;27:4066-4076. https://doi.org/10.1158/1078-0432.CCR-21-0423

12 Kishikawa S, Hayashi T, Saito T, et al. Diffuse expression of MUC6 defines a distinct clinicopathological subset of pulmonary invasive mucinous adenocarcinoma. Mod Pathol 2021;34:786-797. https://doi.org/10.1038/s41379-020-00690-w

13 Board E. Female genital tumours. International Agency for Research on Cancer. Lyon: IARC Press 2020.

14 Mesbah Ardakani N, Giardina T, Amanuel B, et al. Molecular profiling reveals a clonal relationship between ovarian mucinous tumors and corresponding mural carcinomatous nodules. Am J Surg Pathol 2017;41:1261-1266 https://doi.org/10.1097/PAS.0000000000000875

15 Loret N, Denys H, Tummers P, et al. the role of epithelial-to-mesenchymal plasticity in ovarian cancer progression and therapy resistance. Cancers (Basel) 2019;11. https://doi.org/10.3390/cancers11060838

16 Yao D, Dai C, Peng S. Mechanism of the mesenchymal-epithelial transition and its relationship with metastatic tumor formation. Mol Cancer Res 2011;9:1608-1620. https://doi.org/10.1158/1541-7786.MCR-10-0568

17 Skoulidis F, Byers LA, Diao L, et al. Co-occurring genomic alterations define major subsets of KRAS-mutant lung adenocarcinoma with distinct biology, immune profiles, and therapeutic vulnerabilities. Cancer Discov 2015;5:860-877. https://doi.org/10.1158/2159-8290.CD-14-1236

18 Righi L, Vatrano S, Di Nicolantonio F, et al. retrospective multi-center study investigating the role of targeted next-generation sequencing of selected cancer genes in mucinous adenocarcinoma of the lung. J Thorac Oncol 2016;11:504-515. https://doi.org/10.1016/j.jtho.2016.01.004

19 Cha YJ, Shim HS. Biology of invasive mucinous adenocarcinoma of the lung. Transl Lung Cancer Res 2017;6:508-512. https://doi.org/10.21037/tlcr.2017.06.10